Journal of Hazardous Materials 175 (2010) 754–761

Contents lists available at ScienceDirect

Journal of Hazardous Materials

journal homepage: www.elsevier.com/locate/jhazmat

TG–FTIR characterization of pyrolysis of waste mixtures of paint and tar slag

Ling Tao*, Guang-Bo Zhao, Juan Qian, Yu-kun Qin

School of Energy Science and Engineering, Harbin Institute of Technology, 92, West Dazhi Street, Harbin, 150001, PR China

ARTICLE INFO

Article history:
Received 28 July 2009
Received in revised form 20 October 2009
Accepted 20 October 2009
Available online 30 October 2009

Keywords:
Hazardous waste
Pyrolysis
TG–FTIR analysis

ABSTRACT

Safe disposal of hazardous waste is becoming generally more important as industrial production increases. The pyrolysis characteristics and gas evolution of mixtures of several wastes are discussed in this paper. Experiments are described for various heating rates, particle sizes and final temperatures using thermogravimetric analysis (TGA) and a Fourier transform infrared spectrometer. The results indicate that there are three stages in the pyrolysis process. The composition of evolved gas includes carbon monoxide, carbon dioxide, ammonia, methane, nitric oxide, hydrocyanic acid and a number of other light alkanes. Gas evolution temperatures and gas generation rates were significantly influenced by the factors identified.

1. Introduction

Hazardous waste from industrial production is becoming an ever increasing concern as economic development progress. It has been estimated that 10 million ton of hazardous waste is produced annually in China [1–4]. There are a wide variety of industrial hazardous wastes, most of which are harmful and very slow to decompose by natural processes. These various wastes cause great damage to life and the environment and therefore the development of proper waste treatment processes is urgently needed.

In many countries, resource utilization, minimization and harmless treatment are important methods used for disposing of hazardous waste. In China, at present, harmless treatment is the most suitable method. Incineration is widely used because of its ability to minimize and disinfect waste and the low levels of secondary pollution [5]. Incineration has another vantage that combustion of organic composition in waste would release energy, which we can collect by a waste heat boiler. Some waste has higher heating value than coal. Pyrolysis is the leading process of incineration and therefore it should be studied more deeply to gain a better understanding of incineration kinetics and the characteristics of evolved gases. Pyrolysis of solid wastes is a thermo-chemical process based on the poor thermo-stability of the organic components, which decomposes wastes, in an inert gas atmosphere, into solid residues of smaller molecules and combustible gases. Thermogravimetric analysis (TGA) coupled with Fourier transform infrared (FTIR) analysis is widely used to study coal and biomass pyrolysis characteristics, reaction mechanisms and evolved products but it is seldom used for hazardous wastes [6–12]. In this paper, experiments carried out by non-isothermal TGA, coupled with an FTIR spectrometer, are described and the pyrolysis characteristics and evolved products of hazardous wastes derived from paint and tar are identified. Effects of particle size, heating rate and final temperature on pyrolysis characteristics and evolution rules for gaseous products are discussed. Comparison between waste and some coals are also discussed, as some incinerator is transformed by coal boilers, which can help engineers do the transformation.

2. Experimental

2.1. Instrumentation

A Mettler-Toledo thermogravimetric analyzer TGA/SDTA851^e (Mettler-Toledo Instruments Ltd., Shanghai, China) was used in this work [13].

A Thermo Electron Corporation Fourier Transformation Infrared spectrometer Nicolet 5700 was used to collect evolved gases from the thermogravimetric analyzer. The dynamic adjustment of the digital interferometer in the FTIR was 130,000 Hz and the signal to noise ratio was up to 50,000:1. A DTGS-KBr detector was used with a spectrum range of 4000–650 cm^{-1}. The gas cell volume was 2 L.

The TGA and FTIR were connected by a pipe, heated to 120 °C. Fig. 1 illustrates the TGA–FTIR system. The heated pipe was approximately 2 m in length and the gas time delay between the TGA and the FTIR was 8 s. The flow rate of evolved gas was approximately 160 mL/min. Because of the significant volume difference between the flow rate of the evolved gas and the volume of the gas cell, evolved gas would gather in the cell, causing the concentration in the cell to be larger than the actual concentration of the evolved gas. To avoid this problem, a dilution gas of 99.99% nitrogen was

* Corresponding author. Tel.: +86 451 86412908 534; fax: +86 451 86412528.
E-mail address: taolingsd@yahoo.com.cn (L. Tao).

0304-3894/$ – see front matter © 2009 Elsevier B.V. All rights reserved.
doi:10.1016/j.jhazmat.2009.10.073

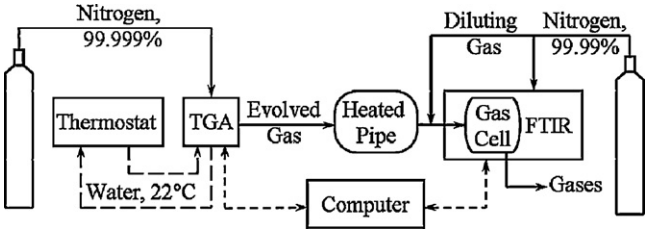

Fig. 1. The system of TGA coupled with FTIR.

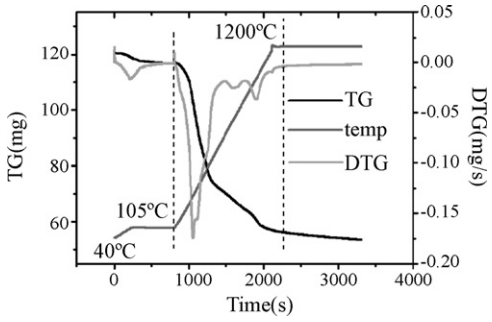

Fig. 2. TG/DTG profiles for test condition 2560-50-1200.

used to increase the flow rate through the cell. The flow rate of the dilution gas was 840 mL/min.

2.2. Specimen and experimental process

The preparation of specimen and the heating process was described in reference [13]. Table 1 provides the elemental composition and heating value of specimen and some other coals. Comparing waste and coals, we can see that waste has too many volatiles. Almost all volatiles are released during the pyrolysis. Thus, the research of pyrolysis and gas release is pretty important.

During experiments, nitrogen with a purity of 99.999% was used as a purge gas at a flow rate of 30 mL/min and as a reactive gas when delivered at a flow rate of 130 mL/min. The temperature of the gas cell was 150 °C. The mass of the specimen was set at about 120 mg. Before starting an experiment, the furnace, the heated pipe and the gas cell were purged for at least 30 min. The FTIR background was measured and recorded after the system was at steady state. The TGA and FTIR experiments were then begun simultaneously. Mass and spectra were recorded over time by the computer. Test conditions for each experimental test of a specimen are referred to below in the format "particle size-heating rate-final temperature".

3. Results and discussion

3.1. Thermogravimetric analysis

The TG/DTG profiles of test condition 2560-50-1200 are presented in Fig. 2. The pyrolysis of wastes could be divided into three stages. The first stage corresponded to a heating period between 40 and 105 °C and an isothermal regime at 105 °C, when the specimen lost its external moisture. The second heating period from 105 to 1200 °C was the main pyrolysis stage, with a large gas evolution, which was the emphasis of this work. The constant temperature stage at 1200 °C was the residual pyrolysis stage, with a small amount of weight loss. From the DTG profile, we found that there were three obvious peaks in the main pyrolysis stage, corresponding to temperatures of 302.3, 752.2 and 1079.4 °C. The first peak was the biggest, the middle one was slight and the last one was medium. Characteristic temperatures rose with increasing particle size. The initial weight loss temperature clearly reduced with increased heating rate while the initial pyrolysis temperature, the maximum weight loss rate temperature, and the finished temperature rose with increased heating rate. Pyrolysis yields increased with increasing final temperature and particle size [13].

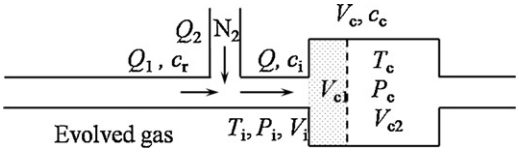

Fig. 3. Diagram of gas flow and gas state in heated pipe and gas cell.

3.2. Gas composition analysis

FTIR has been widely used to identify various inorganic and organic compounds of pyrolysis. The 3D infrared spectrum of evolved gas includes information on infrared absorbance, wave number and time. After evolved gas from TGA was swept into the gas cell, absorbance information at various wave numbers and times could be obtained by FTIR. When time was fixed, absorbance information at various wave numbers could be obtained to analyze the composition of the gas. When wave number was fixed, absorbance information at various times could be obtained to analyze a given composition as a function of time.

3.2.1. Transformation of gas concentration between TGA and FTIR

As a first approximation, the concentration we obtained from the FTIR was the concentration in the cell. However, the gas concentration in the gas cell and that in the heated pipe were not truly identical. First, there was a time delay as gas flowed through the heated pipe. Second, gas measured in the cell at time t was a mixture of all gas before time t. The time delay from the furnace outlet to the cell inlet was approximately 8 s. The relationship of the concentration between the cell and the heated pipe is given in Fig. 3.

We assumed that: (1) gas flowing into the cell and residual gas in the cell at time t would be uniformly mixed at the moment the gas entered the cell, (2) gases in the heated pipe and the cell were considered as ideal, (3) the heated pipe and the cell were at atmospheric pressure, (4) gas concentrations flowing into the cell in the short time period Δt would not change, (5) there was a special membrane in the cell that was conductive.

Table 1
Approximate and ultimate analysis of the specimen.

	V_{daf} (%)	FC_{ar} (%)	C_{ar} (%)	H_{ar} (%)	O_{ar} (%)	N_{ar} (%)	S_{ar} (%)	M_{ar} (%)	A_{ar} (%)	$Q_{net,ar}$ (kJ/kg)
Paint slag	96.32	1.78	36.46	3.91	6.22	1.28	0.19	21.85	30.09	15,183
Tar slag	77.08	20.88	84.27	4.28	1.18	0.82	0.55	7.60	1.30	32,717
Specimen	86.19	1.66	47.87	3.55	6.66	0.81	0.28	19.88	20.95	18,874
Datong coal	24.70	44.56	70.83	4.51	7.09	0.72	2.15	3.02	11.68	27,800
Fengguang coal	55.00	23.54	35.28	3.21	12.57	1.12	0.22	22.01	25.69	13,410
Yangquan coal	9.00	69.14	68.92	2.85	2.42	1.01	0.78	5.03	18.99	26,400

The temperature of the cell was t_c and the gas flow rate was Q, which involved diluting gas Q_1 and released gas Q_2. The volume and the temperature of the gas entering the cell during time period Δt were V_i and T_i, respectively, and the volume expanded at a fixed pressure to V_{c1}. Some gas at time t exited the cell and the volume of the residual gas at time $(t+\Delta t)$ was V_{c2}. The following equations were obtained from the above description.

$$V_i = Q \cdot \Delta t \tag{1}$$

$$V_c = V_{c1} + V_{c2} \tag{2}$$

The following equation is the ideal gas state equation of the gas flowing into the cell during the time period Δt.

$$\frac{T_i}{T_c} = \frac{V_i}{V_{c1}} \tag{3}$$

Substituting Eq. (1) and Eq. (2) into Eq. (3), we obtain the following equation.

$$V_{c1} = \frac{T_c V_i}{T_i} = \frac{T_c Q \Delta t}{T_i} \tag{4}$$

The relationship of the concentration between time t and time $(t+\Delta t)$: the concentration of gas X at time t was $c_c(t)$. The gas reduced to V_{c2} in volume at time $(t+\Delta t)$. Gas X with a concentration $c_i(t)$ and a volume V_i flowed into the cell in the time period Δt and changed volume to V_{c1}. The concentration of gas X in the cell at time $(t+\Delta t)$ was $c_c(t+\Delta t)$. Then, the equation for gas X could be obtained (X was a specific gas).

$$V_c c_c(t+\Delta t) = V_{c1} c_c(t) + V_{c2} c_i(t) \tag{5}$$

Eq. (5) could be changed into the following:

$$V_c \frac{c_c(t+\Delta t) - c_c(t)}{\Delta t} = (c_i(t) - c_c(t)) \frac{Q T_c}{T_i} \tag{6}$$

Taking the limit as Δt approaches zero (Eq. (7)), yields the differential equation, Eq. (8).

$$\lim_{\Delta t \to 0} \left(V_c \frac{c_c(t+\Delta t) - c_c(t)}{\Delta t} \right) = \lim_{\Delta t \to 0} \left((c_i(t) - c_c(t)) \frac{Q T_c}{T_i} \right) \tag{7}$$

$$c_i(t) = c_c(t) + \frac{V_c T_i}{T_c Q} c_c'(t) \tag{8}$$

We know that there was a diluting gas between the TGA and FTIR and $c_i(t)$ was the concentration of gas after dilution. The concentration of evolved gas could therefore be obtained as follows.

$$c_r(t) = \frac{Q}{Q_1} c_i(t) = \frac{Q_1 + Q_2}{Q_1} c_i(t) \tag{9}$$

3.2.2. Analysis of gas composition

Before looking at the spectrum, it should be noted that the concentration of a gas component was in proportion to its absorbance. A 3D spectrum of test condition 2560-50-1200 is presented in Fig. 4. From this, it can be concluded that most of the gas was evolved between 10 and 30 min. Let us take some typical spectra as examples. Five spectra were selected for our primary analysis, as in Fig. 5. Carbon dioxide has a wave number 2400–2260 cm^{-1} and carbon monoxide has a wave number 2260–1990 cm^{-1} in spectrum E. Mainly water vapor was present in wave numbers 4000–3400 cm^{-1} and 2060–1260 cm^{-1}. Two narrow bands at about 964 and 927 cm^{-1} that appeared in the five spectra were the significant peaks of ammonia. The narrow band at 3014 cm^{-1} in spectrum C indicates the existence of methane. Figs. 4 and 5 show that there was almost no carbon dioxide in the evolved gas before 15 min. However, carbon dioxide absorbance increased quickly and reached a peak at 19.45 min and then decreased to a low value by 31 min and held that value for an extended time, as in Fig. 6(a). Carbon dioxide came from the decomposition of carboxyl. At high temperature, some carbonate and oxygen-containing functional groups decomposed. For carbon monoxide, the evolution was much more complicated. No carbon monoxide was evolved before 15 min. However, a very rapid increase in carbon monoxide was then observed and the first peak appeared at 20 min. Carbon monoxide evolution then decreased until 24 min. A second peak of carbon monoxide was observed at 28.5 min and a third peak at 32.5 min. After that, evolution of carbon monoxide decreased rapidly until about 40 min and then reduced more slowly until 56 min, as shown in Fig. 6(b). Carbon monoxide was the decomposition product of quinone ether and the oxygen-containing heterocyclic ring. Carbon dioxide reacted with char at high temperature, which also formed carbon monoxide. Evolution of ammonia was simpler than carbon dioxide and carbon monoxide, starting at about 16 min and reaching a peak at 20 min. The evolution then decreased until 35 min but a tiny gas evolution was still found, as in Fig. 6(c). The formation of ammonia depended on two factors: cleavage of nitrogen heterocyclic rings and the amount of hydrogen free radicals. The evolution of methane was also simple, starting at 16 min and reaching a peak at 22 min. The evolution of methane was similar to that of ammonia, while methane was evolved a little later than ammonia. Below 30 min, the evolution of methane was almost complete and only a little methane separated out from then on, as in Fig. 6(d). The generation of methane depended on the cleavage of fat chains and aromatic side chains with methyl groups. Water was a special component that could be found in the whole spectra. First, water existing in the furnace and heated pipe would flow into the gas cell. Second, moisture condensed out at low temperatures. Third, water would be produced throughout the whole reaction process [14]. Nitric oxide could also be found in the spectrum between 15 and 35 min, with characteristic bands at 1905 and 1849 cm^{-1}. HCN was also found between 16 and 36 min, with characteristic bands at 3342, 3280 and 1435 cm^{-1}. The last characteristic band was covered by bands of water vapor. Additional absorption bands were observed but we could not identify the gas corresponding to those peaks. However, from the vibration of different groups, we could guess the identity of some gases. Bands at 2968, 2933 and 2879 cm^{-1} probably indicated the existence of light alkanes, such as ethane or propane. There was a clear peak at 715 cm^{-1} between 16 and 33 min but we cannot currently identify its meaning.

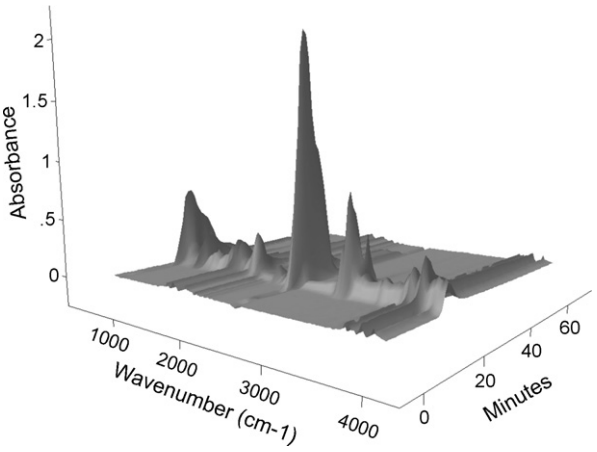

Fig. 4. 3D infrared spectrum for test condition 2560-50-1200.

3.2.3. Quantification of several gases

The FTIR spectrometer cannot give the concentration in the cell, but only give the absorbance as a function of time. To quantify the gas, we did some experiments that we input stable flow of certain gas of different concentrations through the gas cell of FTIR and the corresponding absorbance was measured by the FTIR. Finally,

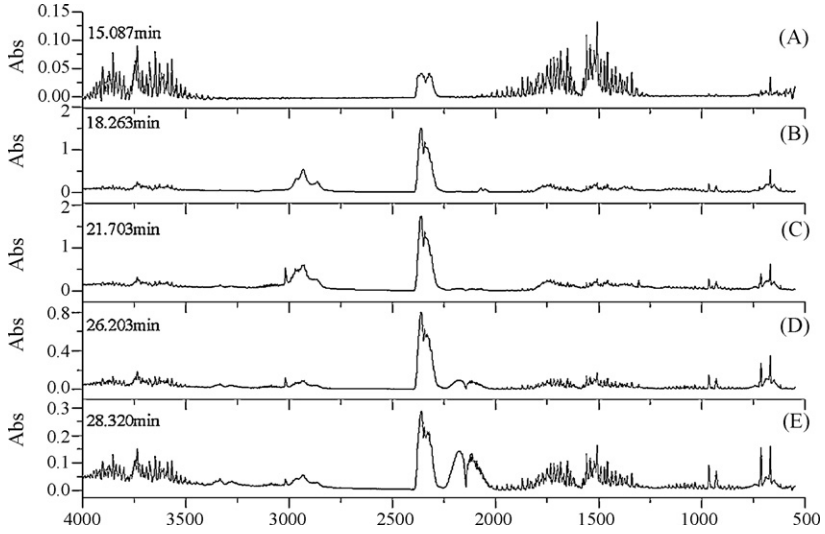

Fig. 5. Typical spectra for test condition 2560-50-1200.

we got a function of measured concentrations and actual concentrations and also a function of absorbances and the corresponding actual concentrations of various gases. Fig. 7 presents the relationship between measured concentrations and actual concentrations while Fig. 8 presents the relationship between concentrations and absorbances of CH_4, NH_3, CO_2, and CO. In Fig. 7, the black line with symbols were the experimental results of actual concentrations and the corresponding measured concentrations while the red lines were the regression lines of the experimental results. In Fig. 8, the black lines with symbols were the experimental results of concentrations and the corresponding absorbances, while the red lines were the regression lines of the experimental results. With these two relationships of concentration and absorbance, the concentration in the cell can be obtained, which means the concentration of evolved gas can also be got, as in Section 3.2.1, with which we can calibrate the total mass of some gases. The calibration process is presented in the following. The total mass of gases can be calibrated from the concentration of evolved gas, as in the following

$$Q_c = Q_1 \cdot c_r(t) \tag{10}$$

where, Q_c is the volume flow of the evolved gas.

$$q_m = \frac{M \cdot Q_c}{V_m} = \frac{M \cdot Q \cdot c_i(t)}{V_m} \tag{11}$$

where, q_m is the mass flow of the evolved gas.

Integrating the mass flow during the whole test process, then the total mass of gas would be obtained.

Fig. 9 shows the gas distribution of test condition 2560-50-1200. We could observe that small amounts of ammonia were produced, which lasted for a long time. The generation of ammonia began at 200 °C and finished at about 800 °C. The generation of methane was more concentrated than the other gases, starting at 305 °C, finish-

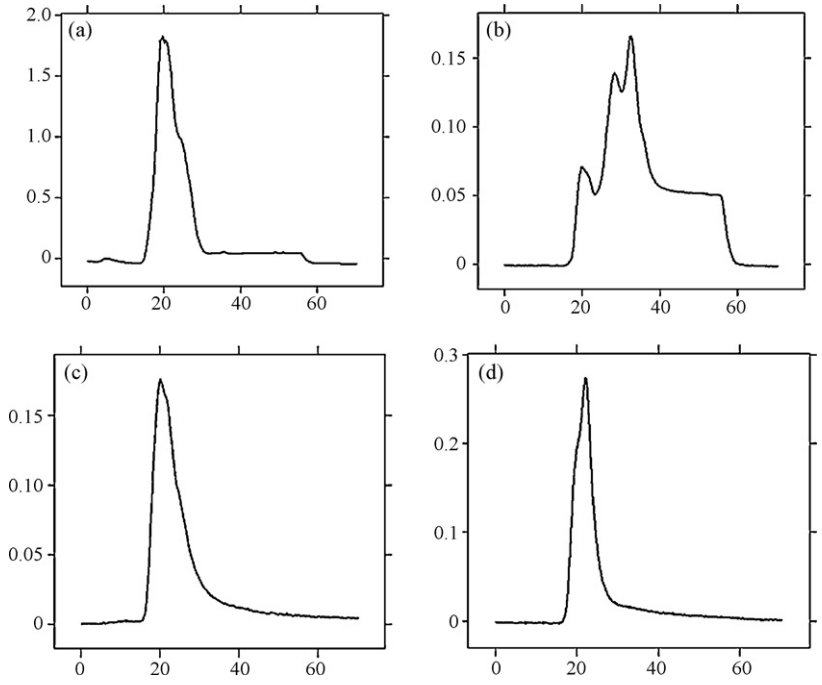

Fig. 6. Absorbance of CO_2, CO, NH_3 and CH_4 during the pyrolysis process.

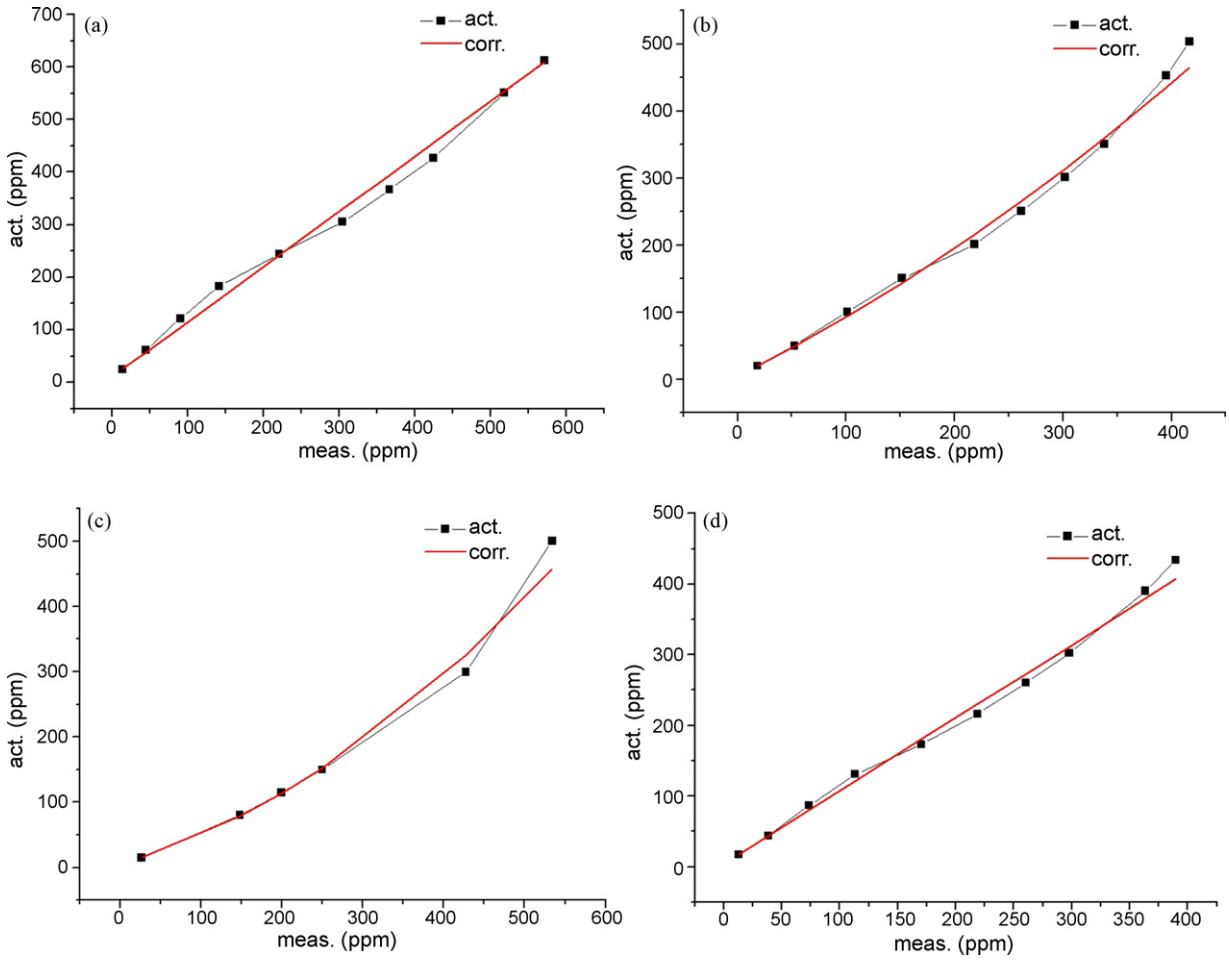

Fig. 7. The relationship between measured concentration and actual concentration of CH_4, NH_3, CO_2, and CO.

ing at 670 °C and reaching a maximum evolution rate at 507 °C. The specimen reached the maximum methane evolution rate earlier than most coals [15]. Carbon monoxide and carbon dioxide were the main pyrolysis gases. Carbon dioxide was observed between 150 and 800 °C and mainly observed at lower temperature, which was similar to pyrolysis of Hegang, Datong and Huolinhe coals [16]. Carbon monoxide generation began at 300 °C and lasted for the whole process. Two peaks of carbon monoxide were found at 786 and 1004 °C. There was a clear flat form in the isothermal stage, perhaps caused by a secondary reaction of carbon dioxide and char [17]. These temperature ranges of the gas evolution are in accordance with the three weight loss stages and weight loss peaks.

3.2.4. *Influences of experimental conditions on gas evolution*

Experiments were carried out at various heating rates, final temperatures and particle sizes. These factors not only affected the evolution temperature but also the quantity of gases. The gas generation rate was defined as the ratio of the mass of gas produced during the whole pyrolysis to the initial specimen mass and was used to evaluate the influences of various factors.

Fig. 10 shows the generation rates of methane, ammonia, carbon dioxide and carbon monoxide at various final temperatures on a particle size 0.25–0.60 mm at a heating rate of 50 °C/min. The results show that the final temperature had differing influences on different gases. The final temperature had no effect on methane generation but ammonia generation increased with increasing final temperature. Ammonia generation mainly depended on two factors: cleavage of the nitrogen bond and the source of H free radicals. Polycondensation occurred at high temperatures and released H free radicals. Higher final temperatures resulted in more polycondensation and more H free radicals. Generation of carbon dioxide was complex. It increased initially and then decreased with an increase in the final temperature. Below 1000 °C, carbon dioxide increased with an increase in final temperature. This was because a higher final temperature caused more decomposition of macromolecules and so more carbon dioxide was formed. However, there was less carbon dioxide released when the final temperature was higher than 1000 °C. This was because some carbon dioxide reacted with char at high temperatures and produced carbon monoxide. Carbon monoxide increased significantly with an increase in final temperature. First, decomposition of macromolecules would increase with the increase in final temperature. Second, secondary reactions would have occurred at such high temperatures. An important mechanism for carbon monoxide formation was the reaction between carbon dioxide and char. We can conclude that the weight loss of specimen higher than 800 °C was significantly caused by the evolution of carbon monoxide and carbon dioxide.

Influences of heating rate on gas generation are presented in Fig. 11. These test conditions were carried out on particle sizes 0.25–0.60 mm and a final temperature of 1200 °C. It is clear that all gas generation rates decreased with an increase in heating rate. This behavior could also be explained by temperature hysteresis and pyrolysis hysteresis [13]. A higher heating rate shortened the time period for gas evolution and there were more bonds polymerized to form larger and more stable macromolecules.

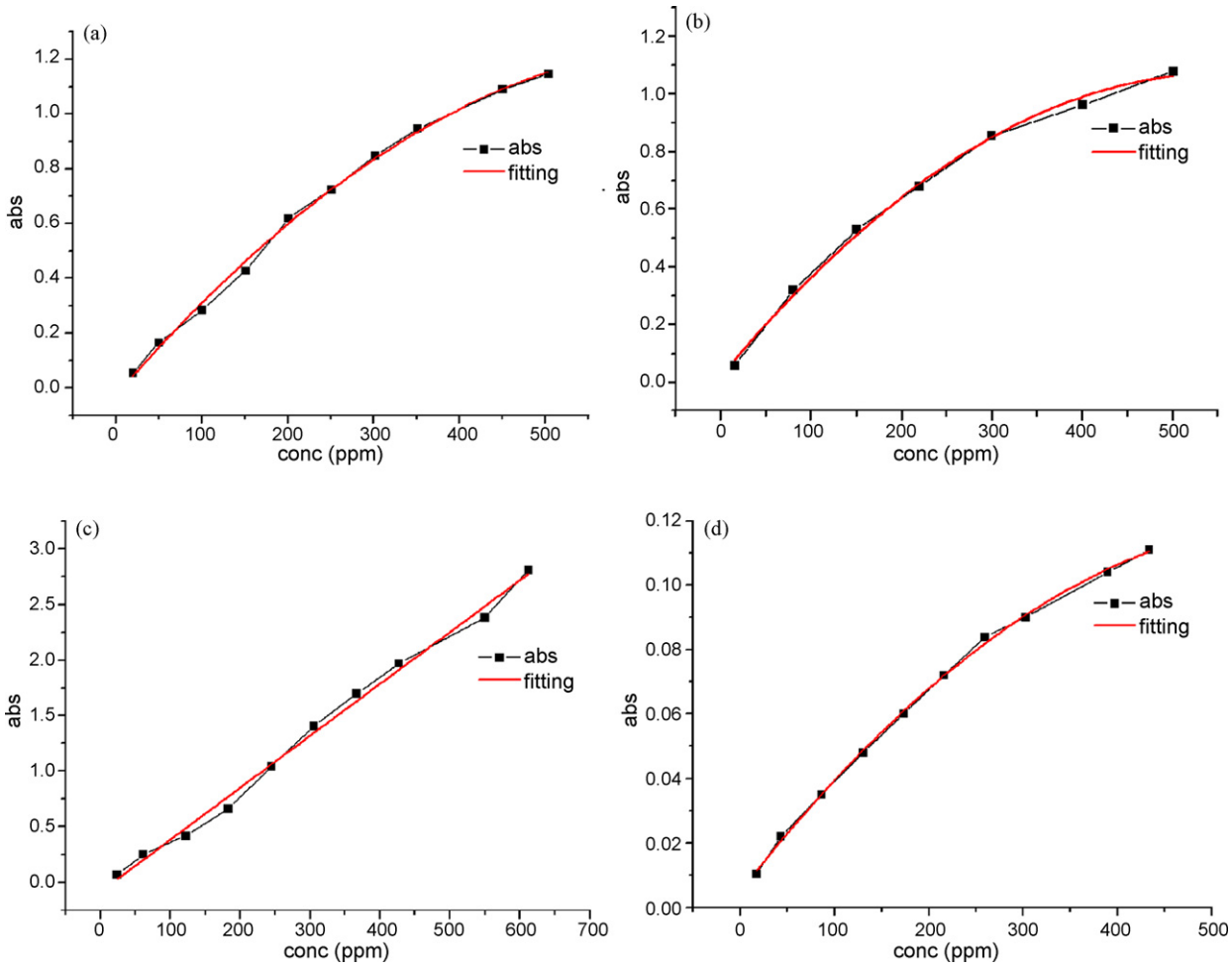

Fig. 8. The relationship between concentration and absorbance of CH_4, NH_3, CO_2, and CO.

Fig. 12 shows the gas generation rate of various particle sizes at a final temperature of 1200 °C and a heating rate of 50 °C/min. Three behaviors were observed: methane decreased slightly with an increase in particle size; carbon dioxide and carbon monoxide increased with an increase in particle size; and generation of ammonia had no clear rules. The decrease in methane could be explained by the following reasoning. The temperature gradient was small and the entire particle was therefore heated rapidly when the particle size was small. Therefore, gases could separate out over time. Ammonia generation had no clear rules. This might have been caused by the following factors. First, ammonia was present in low amounts, so that large errors might be produced during the quantification. Second, larger particle sizes caused higher diffusional resistances, which affected the evolution of ammonia. There was a temperature gradient between the surface and interior of particles, which became larger with an increase in particle size. Pyrolysis occurred from the surface towards the interior, occurring at the surface and forming many small holes where volatiles could separate out easily. Furthermore, larger particles had a larger chance of secondary reaction. Thus, carbon monoxide and carbon dioxide were generated more with an increase in particle size.

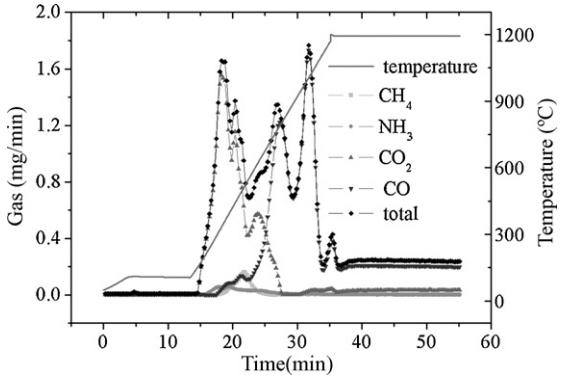

Fig. 9. Evolved gas for test condition 2560-50-1200.

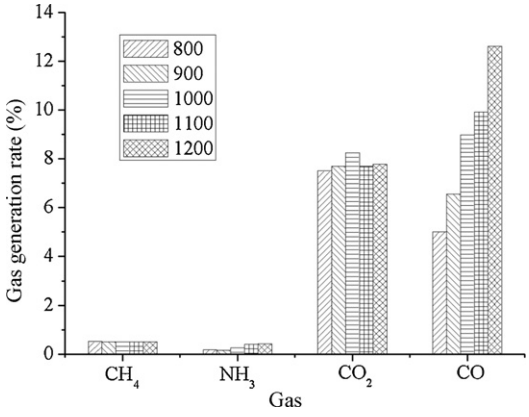

Fig. 10. Generation rates of CH_4, NH_3, CO_2 and CO of various final temperatures.

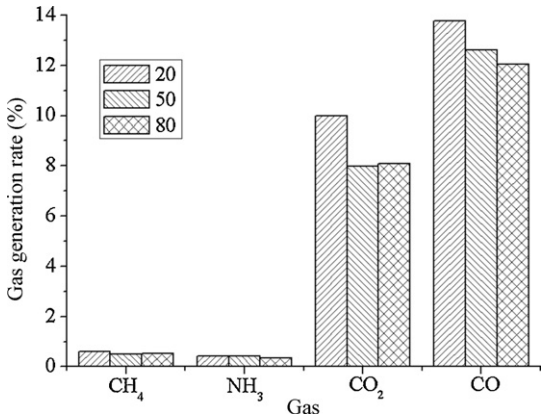

Fig. 11. Generation rates of CH_4, NH_3, CO_2 and CO of various heating rates.

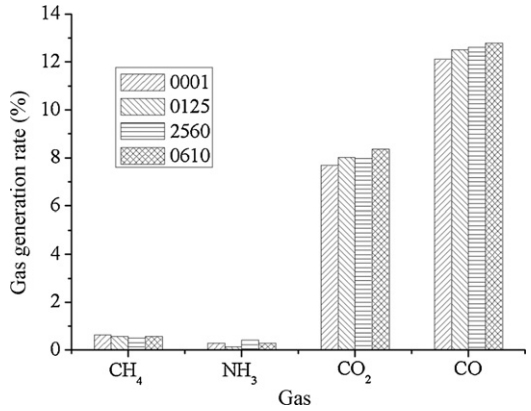

Fig. 12. Generation rates of CH_4, NH_3, CO_2 and CO of various particle sizes.

The maximum evolution temperatures of gases for different test conditions are shown in Table 2. All gases we measured reached a maximum release temperature later with an increase in heating rate [13]. Particle size also had a significant influence on the maximum evolution temperature. The maximum evolution temperatures of methane, ammonia and carbon dioxide decreased with an increase in particle size. The reason for this is clear. Particles were small and the gaps between particles were also small. This caused a greater diffusional resistance, which prevented volatiles from leaving the solid. Therefore, more time was needed to reach the maximum value. However, the maximum evolution temperature of carbon monoxide increased with an increase in particle size. As noted above, significant amounts of carbon monoxide were formed by carbon dioxide and char. The escape of carbon dioxide would inhibit the generation of carbon monoxide and the maximum evolution temperature therefore increased.

Table 2
Max evolution temperatures of gases of various heating rates and particle sizes.

	Heating rate (°C/min)			Particle size			
	20	50	80	0001	0125	2560	0610
CH_4	491.47	507.66	515.75	518.88	506.27	507.66	506.79
NH_3	312.49 417.77	323.30 389.14	347.13 473.59	334.85 426.87	322.20 414.23	323.30 389.14	309.47 401.55
CO_2	301.96 417.77 554.64	336.47 441.82 613.00	347.13 473.59 642.22	334.85 440.01 637.19	335.35 427.38 611.45	336.47 441.82 613.00	335.78 427.86 612.02
CO	754.67 970.50	783.03 1006.65	789.76 1021.62	768.64 1005.25	769.23 1005.89	783.03 1006.65	784.19 1006.65

3.3. Limitations and prospects

Water vapor was found throughout the test process. Water vapor has narrow bands at 2000–1300 and 4000–3500 cm^{-1}, coincident with the bands for other gases. On one hand, the existence of water vapor obscured some other gases that had characteristic bands in these spectrum ranges. On the other hand, if we dried the evolved gas, the fraction of ammonia that reacted with water would also be removed. In this work, water vapor was retained to enable better accuracy of ammonia. Another problem was how to measure water vapor produced by pyrolysis. The standard spectrum of water vapor was too difficult for us to obtain using the experiment system. A third limitation was that hydrogen could not be detected by the FTIR spectrometer.

Further studies should be focused on the following problems. First, the gas composition should be analyzed by gas chromatography because hydrogen and a number of other gases that cannot be detected by FTIR spectrometer. Second, the mechanics of specimen decomposition should be further studied. Finally, the decomposition of a single waste should be carried out in the future for comparison with a mixture of wastes.

4. Conclusions

The pyrolysis of waste mixtures of paint and tar slag was investigated in this study. Experiments at various heating rates, particle sizes and final temperatures were carried out to investigate the pyrolysis characteristics and gas evolution, using TGA–FTIR.

The pyrolysis of wastes could be divided into three stages. The first stage was a heating period between 40 and 105 °C and an isothermal regime at 105 °C, when the specimen lost its external moisture. The second heating period from 105 to 1200 °C was the main pyrolysis stage, with a large gas evolution. The constant temperature stage at 1200 °C was the residual pyrolysis stage, with a small amount of weight loss. There were three obvious peaks in the main pyrolysis stage, corresponding to temperatures of 302.3, 752.2 and 1079.4 °C.

For test condition 2560-50-1200, most of the gas was evolved between 10 and 30 min carbon dioxide, carbon monoxide, ammonia, methane, water vapor, nitric oxide, and hydrogen cyanide could be observed from the 3D spectrum. There were also light alkanes, such as ethane or propane in the released gas.

The relationship between concentration and absorbance of several gases was given. The generation of ammonia began at 200 °C and finished at about 800 °C. The generation of methane started at 305 °C, finished at 670 °C and reached a maximum evolution rate at 507 °C. Carbon dioxide was observed between 150 and 800 °C and mainly observed at lower temperature. Carbon monoxide generation began at 300 °C and lasted for the whole process. Two peaks of carbon monoxide were found at 786 and 1004 °C. These temperature ranges of the gas evolution are in accordance with the three weight loss stages and weight loss peaks.

The final temperature had differing influences on different gases. The final temperature had no effect on methane generation but ammonia generation increased with increasing final temperature. Generation of carbon dioxide increased initially and then decreased with an increase in the final temperature. Below 1000 °C, carbon dioxide increased with an increase in final temperature. Carbon monoxide increased significantly with an increase in final temperature.

All gas generation rates decreased with an increase in heating rate. Methane decreased slightly with an increase in particle size; carbon dioxide and carbon monoxide increased with an increase in particle size; and generation of ammonia had no clear rules. The maximum evolution temperatures of methane, ammonia and carbon dioxide decreased with an increase in particle size.

However, the maximum evolution temperature of carbon monoxide increased with an increase in particle size.

References

[1] C.J. Yang, C.Q. Hu, Studies of tar slag utilization, Fuel Chem. Processes 35 (2004) 39–40 (in Chinese).
[2] H.M. Zhu, J.H. Yan, X.G. Jiang, Y.E. Lai, K.F. Cen, Study on pyrolysis of typical medical waste materials by using TG-FTIR analysis, J. Hazard. Mater. 153 (2008) 670–676.
[3] T.H. Liou, Pyrolysis kinetics of electronic packaging material in a nitrogen atmosphere, J. Hazard. Mater. 103 (2003) 107–123.
[4] J.H. Yan, H.M. Zhu, X.G. Jiang, Y. Chi, K.F. Cen, Analysis of volatile species kinetics during typical medical materials pyrolysis using a distributed activation energy model, J. Hazard. Mater. 162 (2009) 646–651.
[5] Z.Q. Liu, J.H. Li, Y.F. Nie, Development trend and policy analysis on prevention and control technology of hazardous waste pollution in China, China Environ. Prot. Ind. 6 (2000) 12–14 (in Chinese).
[6] R. Bassilakis, R.M. Carangelo, M.A. Wójtowicz, TG-FTIR analysis of biomass pyrolysis, Fuel 80 (2001) 1765–1786.
[7] W.D. Jong, G.D. Nola, B.C.H. Venneker, H. Spliethoff, M.A. Wójtowicz, TG-FTIR pyrolysis of coal and secondary biomass fuels: determination of pyrolysis kinetics parameters for main species and NOx precursors, Fuel 86 (2007) 2367–2376.
[8] X.G. Li, B.G. Ma, L. Xu, Z.W. Hu, X.G. Wang, Thermogravimetric analysis of the co-combustion of the blends with high ash and waste tyres, Thermochim. Acta 441 (2006) 79–83.
[9] J.H. Ferrasse, S. Chavez, P. Arlabosse, N. Dupuyc, Chemometrics as a tool for the analysis of evolved gas during the thermo treatment of sewage sludge using coupled TG-FTIR, Thermochim. Acta 404 (2003) 97–108.
[10] S. Li, J. Lyons-Hart, J. Banyasz, K. Shafer, Real-time evolved gas analysis by FTIR method an experimental study of cellulose pyrolysis, Fuel 80 (2001) 1809–1817.
[11] N. Miskolczi, L. Bartha, Investigation of hydrocarbon fractions form waste plastic recycling by FTIR, GC, EDXRFS and SEC techniques, J. Biochem. Biophys. Methods 70 (2008) 1247–1253.
[12] J.P. Charland, J.A. MacPhee, L. Giroux, J.T. Price, M.A. Khan, Application of TG-FTIR to the determination of oxygen content of coals, Fuel Process. Technol. 81 (2003) 211–221.
[13] L. Tao, G.B. Zhao, J. Qian, Thermogravimetric analysis and pyrolysis of waste mixtures of paint and tar slag, Korean J. Chem. Eng. 26 (2009) 856–861.
[14] Y.B. Yang, V.N. Sharifi, J. Swithenbank, Effect of air flow rate and fuel moisture on the burning behaviors of biomass and simulated municipal solid wastes in packed beds, Fuel 83 (2004) 1553–1562.
[15] F.X. Xiong, S.H. Wu, W.G. Lin, Study on Hegang bituminous coal pyrolysis by TG-FTIR, Power Syst. Eng. 22 (2006) 26–28 (in Chinese).
[16] W.P. Jiang, Study on the kinetics and devolatilization of coal pyrolysis, Dalian University of technology, master degree thesis, 2004 (in Chinese).
[17] K.R. Doolan, J.C. Mackie, R.J. Tyler, Coal flash pyrolysis: secondary cracking of tar vapours in the range 870–2000 K, Fuel 66 (1987) 572–578.

Ling Tao is a PhD student at Harbin Institute of Technology, focusing on pyrolysis and combustion characteristics of typical hazardous waste.